Binding kinetics of an anti-dinitrophenyl monoclonal Fab on supported phospholipid monolayers measured by total internal reflection with fluorescence photobleaching recovery

Mary Lee Pisarchick, Diane Gesty, and Nancy L. Thompson
Department of Chemistry, University of North Carolina, Chapel Hill, North Carolina 27599-3290

ABSTRACT Fluorescence photobleaching recovery with total internal reflection illumination (TIR-FPR) has been used to measure the dissociation kinetics of a fluorescein-labeled anti-dinitrophenyl monoclonal Fab specifically bound to supported monolayers composed of a mixture of dipalmitoylphosphatidylcholine and dinitrophenyl-conjugated dipalmitoylphosphatidylethanolamine. The fluorescence recovery curves were not monoexponential; when analyzed as a sum of two exponentials, the rates and fractional recoveries were ≈ 1 s^{-1} ($\approx 50\%$) and ≈ 0.1 s^{-1} ($\approx 30\%$). The data did not change as a function of the Fab solution concentration, indicating that the fluorescence recovery curves were not influenced by the rate of diffusion in bulk solution. Also, the recovery curves were independent of the size of the illuminated area, indicating that surface diffusion did not significantly contribute to the rate and shape of the fluorescence recovery. The measured off rates and apparent association constant (1.6×10^5 M^{-1}) were analyzed with the theoretical formalism for a proposed mechanism that accounts for the nonmonoexponential kinetics.

INTRODUCTION

The association of antibodies with cell surfaces is a key molecular event in antibody-mediated immune mechanisms such as complement activation, phagocytosis, B cell regulation, and antibody-dependent, cell-mediated cytotoxicity. The relationship of the thermodynamic and kinetic aspects of antibody–membrane interactions to the sequence of signals that ultimately lead to these immune responses is not yet well understood. The details of the association of antibodies with surfaces are also of importance in the development and characterization of biosensors and immunodiagnostic devices.

One method of investigating the interaction of antibodies with membrane-like surfaces is to use phospholipid Langmuir-Blodgett monolayers or bilayers deposited on planar substrates (Thompson et al., 1988; McConnell et al., 1986). Previous work has shown that anti-dinitrophenyl (DNP) monoclonal antibodies can bind to these planar model membranes if they contain DNP-conjugated phospholipids. The ability of anti-DNP antibodies to bind to the membrane surfaces and the subsequent spatial arrangements and lateral and rotational mobilities of the bound antibodies are sensitive functions of the physical and chemical properties of the membranes (e.g., Piepenstock and Losche, 1991; Timbs et al., 1991; Timbs and Thompson, 1990; Pisarchick and Thompson, 1990; Tamm, 1988; Subramaniam et al., 1986; Kimura et al., 1986; Uzgiris and Kornberg, 1983). In addition, immunological cells containing surface receptors for antibodies specifically bind to and metabolically respond to antibody-coated supported phospholipid monolayers (Weis et al., 1982; Hafeman et al., 1981).

A technique for quantitatively characterizing the association of fluorescently labeled molecules with supported planar membranes is total internal reflection fluorescence microscopy (TIRFM; Hellen et al., 1988; Axelrod et al., 1984; Mahan and Bitterli, 1978). In this technique, the thin evanescent field created by a totally internally reflected light source selectively excites membrane-bound fluorescent molecules. TIRFM illumination has recently been used to examine the association at apparent equilibrium of a variety of biochemical ligands with specific sites on model membrane surfaces (e.g., Pearce et al., 1992; Poglitsch et al., 1991; Kalb et al., 1990; Tendian et al., 1990; Poglitsch and Thompson, 1990; Hlady et al., 1988/1989; Sui et al., 1988; Darst et al., 1988).

When total internal reflection illumination is combined with fluorescence photobleaching recovery (TIR-FPR), the data contain information about surface binding kinetic rates and/or surface diffusion coefficients (Abney et al., 1992; Thompson et al., 1981). In this technique, surface-bound, fluorescently labeled ligands are bleached by a high intensity pulse of the evanescent field and subsequent fluorescence recovery is monitored as surface-bound, bleached molecules exchange with unbleached molecules in solution. This kinetic method has been applied to only a few model systems, including primarily nonspecific protein absorption on bare or polymer-coated quartz (Zimmerman et al., 1990; Schmidt et al., 1990; Tilton et al., 1990*a, b;* Axelrod et al., 1986; Burghardt and Axelrod, 1981), but also, more recently, to protein binding at model and natural membrane surfaces (Pearce et al., 1992; Hellen and Axelrod, 1991; Weis et al., 1982). Here, TIR-FPR is applied to the binding kinetics of Fabs from a monoclonal anti-DNP antibody (ANO2) at supported phospholipid monolayers containing DNP-conjugated phospholipids.

Dr. Pisarchick's present address is Becton Dickinson Research Center, Research Triangle Park, NC 27709-2016.

MATERIALS AND METHODS

Antibodies

Polyclonal sheep IgG (Sigma Chemical Co., St. Louis, MO) and fluorescein-labeled mouse IgG Fab (Jackson ImmunoResearch, Inc., West Grove, PA) were obtained commercially and dissolved in phosphate-buffered saline (PBS; 0.05 M sodium phosphate, 0.15 M sodium chloride, and 0.01% sodium azide, pH 7.4). The labeled (F-) mouse IgG Fab was further purified with Sephadex G25M chromatography in PBS.

The mouse monoclonal IgG1 anti-DNP antibody ANO2 (Balakrishnan et al., 1982*a*) was purified from hybridoma supernatants by affinity chromatography using DNP-conjugated human serum albumin (DNP-HSA). Antibodies were eluted with 0.01 M *N*-2,4-dinitrophenylglycine (DNP-G) in PBS followed by extensive dialysis against PBS (Pisarchick and Thompson, 1990). ANO2 Fab fragments were prepared by treating intact ANO2 with preactivated (30 min, 37°C) papain in 0.1 M sodium phosphate, 0.01% sodium azide, 10 mM cysteine, and 8 mM EDTA, pH 7.2 at a 1:100 ratio (wt/wt) of papain to ANO2 for 20 h at 37°C. The digestion mixture was quenched with 20 mM iodoacetamide for 1 h at 0°C. The ANO2 Fab fragments were purified from the digestion mixture using gel filtration (Sephadex G75-200, 1.5 cm × 67 cm, 0.3 ml/min, 1 ml sample volume, 25°C) in PBS. SDS-PAGE with silver staining showed that the primary impurity in the digestion mixture was of low molecular weight (<20 kD) and that no detectable intact antibodies were present. The low molecular weight impurities were removed by the gel filtration column.

ANO2 Fab fragments were labeled with fluorescein isothiocyanate (F-; Molecular Probes, Inc., Junction City, OR) by treating 0.6 mg/ml ANO2 Fab in 0.1 M $NaHCO_3/Na_2CO_3$, pH 9.5, with a 66 M excess of dye dissolved in dimethylsulfoxide for 1 h at 25°C. The volume of added dimethylsulfoxide was <5–10% of the total volume. The F-(ANO2 Fab) was further purified by sequential chromatography with Sephadex G50-80 in PBS (to remove unreacted fluorescein), DNP-HSA (to remove digestion products other than DNP-active ANO2 Fabs), Sephadex G50-80 in PBS (to remove the majority of the DNP-G from the elution buffer for the DNP-HSA column), and dialysis against PBS for ~1 wk.

Absorption spectroscopy indicated that <5% of the antigen binding sites remained occupied with DNP-glycine after purification by gel filtration and dialysis. The Fab concentrations and the molar ratios of fluorescein to Fab (0.4–2.5 for ANO2 Fab and 0.4 for mouse IgG Fab) were determined spectrophotometrically (Timbs and Thompson, 1990). The relative fluorescence intensities of different labeled antibody preparations were determined spectrofluorometrically (SLM model 8000C, λ_{ex} = 480, λ_{em} = 495–630, 20 μg/ml).

Supported phospholipid monolayers

Solid-like phospholipid monolayers were composed of dinitrophenylaminocaproyldipalmitoylphosphatidylethanolamine (DNP-cap-DPPE; Avanti Polar Lipids, Inc., Birmingham, AL) and dipalmitoylphosphatidylcholine (DPPC; Calbiochem Corp., La Jolla, CA) (25:75, mol/mol) or of DPPC. Lipids were spread at 100 $Å^2$/molecule on the air/water interface of a Joyce-Loebl Langmuir trough (model 4; Vickers Instruments, Inc., Malden, MA) at room temperature (21–25°C). The monolayers were compressed at 1–3 $Å^2$/molecule per min to a final pressure of 35 dyn/cm and deposited on fused silica microscope slides pretreated with octadecyltrichlorosilane (Aldrich Chemical Co., Milwaukee, IL) by vertical dipping at ≈5 mm/min (Timbs et al., 1991).

All antibodies were clarified by 0.22-μm filtration and sedimentation at 134,000 *g* for 30 min before use with supported monolayers. Samples were prepared for fluorescence microscopy by treating supported monolayers in PBS with 100 μl of 1 mg/ml sheep IgG/PBS for 5 min to block nonspecific binding sites and then with 200 μl of F-(ANO2 Fab) or F-(mouse IgG Fab) containing 1 mg/ml sheep IgG/PBS for at least 15 min. In some control measurements the final solution contained 100 μM DNP-G, which was sufficient to saturate most of the ANO2 hapten-binding sites in that the ANO2 solution association constant for DNP-G is $3 \times 10^6\ M^{-1}$ (Pisarchick and Thompson, 1990). In other control measurements, monolayers first treated with 200 μl of 1 μM F-(ANO2 Fab) (and 1 mg/ml sheep IgG) were subsequently washed with 200 μl of 3 μM ANO2 Fab in PBS.

Fluorescence microscopy

The fluorescence arising from labeled antibodies on supported monolayers was measured with TIRFM as described (Pisarchick and Thompson, 1990), with the following conditions: wavelength, 488 nm; angle of incidence on the monolayer/solution interface, 75°; laser power, 30 μW; size of the illuminated area, 50 × 200 μm; temperature, 25–28°C. For these conditions and with the refractive indices of the quartz substrate and solution approximately equal to 1.47 and 1.33, respectively, the depth of the evanescent intensity is $d \approx 820$ Å (Pearce et al., 1992). TIR-FPR recovery curves using evanescent illumination were obtained as described (Burghardt and Axelrod, 1981), with the following additional parameters: size of the illuminated area, 50 × 200 or 200 × 550 μm; bleaching power, 0.5 W; bleaching duration, 50–200 ms; bleaching depth, 30–100%. Equilibrium binding curves and TIR-FPR recovery curves were fit to functional forms using the nonlinear Gauss-Newton routine in the ASYST software system (Asyst Software Technologies, Rochester, NY).

RESULTS AND DISCUSSION

Equilibrium binding of F-(ANO2 Fab) to supported monolayers

Monolayers composed of DNP-cap-DPPE/DPPC (25:75, mol/mol) or DPPC were deposited on octadecyltrichlorosilane-treated fused silica. Previous work has shown that these monolayers, when doped with fluorescent lipid probes, are uniformly fluorescent within optical resolution, and that ≤10% of the fluorescent lipids are laterally mobile with an apparent diffusion coefficient $\leq 5 \times 10^{-10}$ cm^2/s (Pisarchick and Thompson, 1990).

The association at equilibrium of F-(ANO2 Fab) with DNP-cap-DPPE/DPPC and DPPC monolayers was examined with steady-state TIRFM. The bound F-(ANO2 Fab) was uniformly distributed on DNP-cap-DPPE monolayers within optical resolution. The evanescently excited fluorescence of F-ANO2 Fab, quantitatively measured as a function of the Fab solution concentration, had the general appearance of a conventional saturation curve (Fig. 1). In contrast, the fluorescence of F-(ANO2 Fab) on DPPC monolayers was lower and linear with the Fab solution concentration (data not shown). The fluorescence of two other types of control samples, F-(mouse IgG Fab) on DNP-cap-DPPE/DPPC monolayers and F-(ANO2 Fab) on DNP-cap-DPPE/DPPC monolayers in the presence of saturating amounts of DNP-G, was also much lower than the fluorescence of F-(ANO2 Fab) on DNP-cap-DPPE/DPPC monolayers (Table 1). These results suggest that the majority of the measured fluorescence of F-(ANO2 Fab) on DNP-cap-DPPE/DPPC monolayers arose from Fabs specifically bound to the monolayers through their hapten-binding regions, consistent with previous results (Pisarchick and Thompson, 1990).

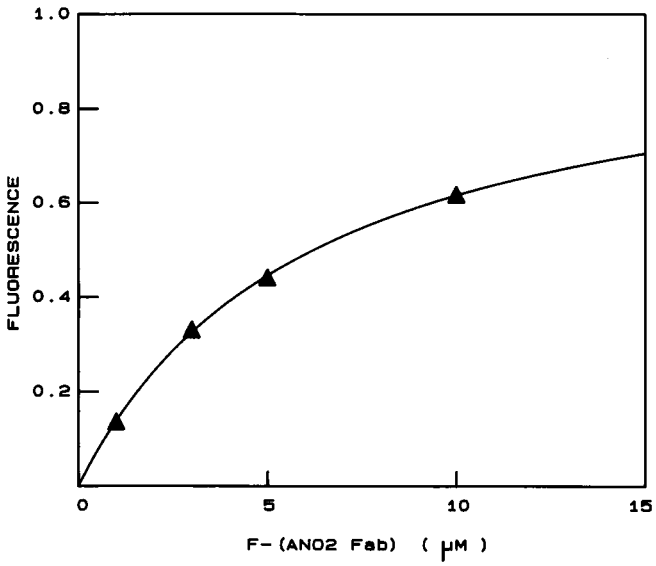

FIGURE 1 F-(ANO2 Fab) binding to DNP-cap-DPPE/DPPC monolayers. The evanescently excited fluorescence of F-(ANO2 Fab) on DNP-cap-DPPE/DPPC monolayers increased and began to saturate with increasing solution concentrations of F-(ANO2 Fab). The standard errors in the mean are smaller than the size of the plotted points. The best fit of the data for DNP-cap-DPPE/DPPC monolayers to Eq. 2 (*line*) was for $K = 1.6 \times 10^5\ M^{-1}$. The data have been normalized by the best-fit value of $F(\infty)$.

The reversibility of F-(ANO2 Fab) surface association was tested by washing monolayers containing bound F-(ANO2 Fab) with solutions containing unlabeled ANO2 Fabs. When monolayers treated with 1 μM F-(ANO2 Fab) were treated with a solution containing 3 μM unlabeled ANO2 Fab, the evanescently excited fluorescence was almost completely abolished (i.e., reduced by ≈95%) relative to the prewash fluorescence intensity.

The fraction of the evanescently excited fluorescence that arose from bound F-(ANO2 Fab) rather than from F-(ANO2 Fab) in solution but close enough to the surface to be excited by the evanescent field was determined by measuring the bleachable fraction (Schmidt et al., 1990) using TIR-FPR (Thompson et al., 1981; Burghardt and Axelrod, 1981). For 2.6 μM F-(ANO2 Fab) on DNP-cap-DPPE/DPPC monolayers, ~90–100% of the evanescently excited fluorescence was bleachable, whereas, in the presence of 100 μM DNP-G, ~80–90% was bleachable. These results indicate that the majority of the measured fluorescence on both types of monolayer surfaces was due to F-(ANO2 Fab) that was membrane bound, rather than in solution but within the finite depth of the evanescent field. Although some weak, nonspecific adsorption to the monolayer surfaces presumably occurred even when the F-(ANO2 Fab) hapten-binding sites were occupied, consistent with other reports (Piepenstock et al., 1991), the measured fluorescence in the absence of soluble hapten was much higher, indicating that the majority of the bound F-(ANO2 Fab) in the absence of DNP-G was attached to the surface via the antigen binding region.

The measured fluorescence for F-(ANO2 Fab) on DNP-cap-DPPE/DPPC monolayers was taken to be proportional to the density of bound F-(ANO2 Fab) (Pisarchick and Thompson, 1990). The apparent surface association constant was obtained from the measured dependence of the fluorescence on the F-(ANO2 Fab) solution concentration. The simplest surface reaction may be modeled as a reversible bimolecular reaction between the Fabs in solution and haptens on the surface, i.e.,

$$A + B \underset{k_{off}}{\overset{k_{on}}{\rightleftharpoons}} C \tag{1a}$$

$$K = \frac{k_{on}}{k_{off}} = \frac{C}{AB} \tag{1b}$$

where C and B are the two-dimensional densities of bound (occupied) and free (unoccupied) surface binding sites, A is the ligand solution concentration, K is the apparent association constant, and k_{on} and k_{off} are the association and dissociation kinetic rates. The dependence of the fluorescence, F, on the ligand solution concentration, A, for this mechanism is

$$F(A) = \frac{F(\infty)KA}{1 + KA} \tag{2}$$

where $F(\infty)$ is the fluorescence when the F-(ANO2 Fab) solution concentration is infinite.

Curve fitting the measured values of $F(A)$ to the form of Eq. 2 with K and $F(\infty)$ as free parameters gave $K = 1.6 \times 10^5\ M^{-1}$. This value is consistent with a previous and more thorough measurement of the apparent association constant for tetramethylrhodamine-labeled ANO2 Fab on DNP-cap-DPPE monolayers (Pisarchick and Thompson, 1990). This previous work also showed that ANO2 Fab adsorption to the monolayers reached apparent equilibrium after ~15 min, and that the ANO2 Fab

TABLE 1 TIRFM fluorescence intensities

Ligand	Monolayer composition	DNP-G (100 μM)	Fluorescence (10^3 photons/s)
F-(ANO2 Fab)	DNP-cap-DPPE/DPPC	no	29.3 ± 2.4
F-(ANO2 Fab)	DNP-cap-DPPE/DPPC	yes	6.1 ± 1.8
F-(ANO2 Fab)	DPPC	no	7.7 ± 0.6
F-(mouse IgG Fab)	DNP-cap-DPPE/DPPC	no	4.6 ± 0.3

The evanescently excited fluorescence of labeled Fabs on supported monolayers was approximately fivefold higher for F-(ANO2 Fab) on DNP-cap-DPPE/DPPC monolayers as compared to the control samples. The antibody solution concentrations were 2.6 μM. The measured fluorescence intensities were corrected for background intensity and the relative fluorescence of different labeled antibody preparations. Values are averages over nine or more measurements on each of two or three independently prepared samples. Errors are standard deviations.

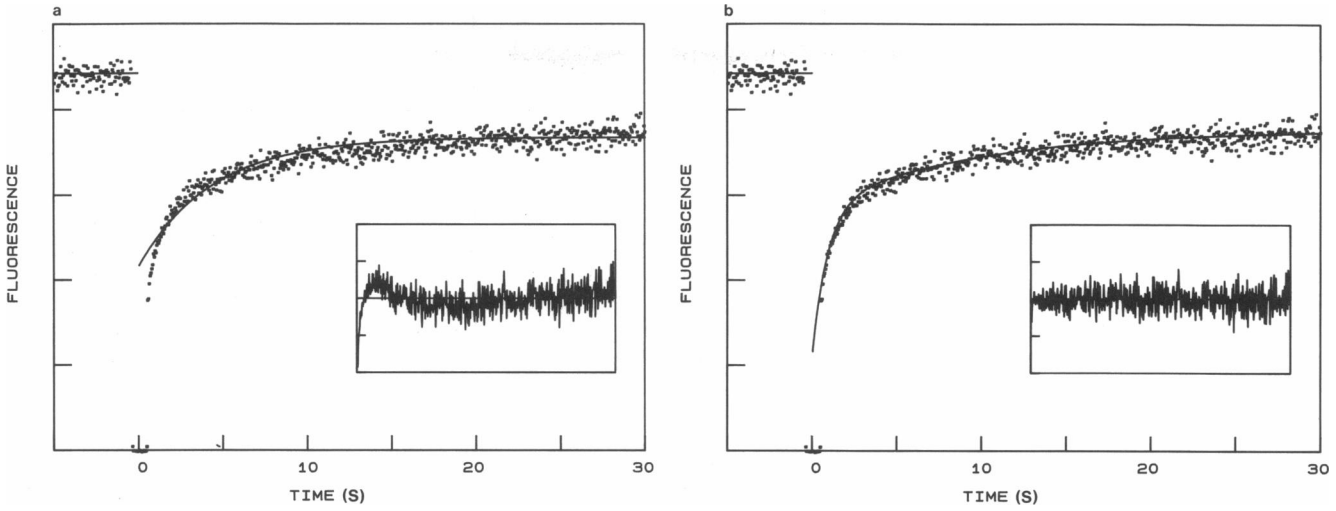

FIGURE 2 TIR-FPR recovery curves for F-(ANO2 Fab) on DNP-cap-DPPE/DPPC monolayers. A typical recovery curve for 3 μM F-(ANO2 Fab) on DNP-cap-DPPE/DPPC monolayers is compared to the best fits to Eq. 4 with (*a*) $n = 1$ and (*b*) $n = 2$. The residuals are shown in the insets.

solution concentrations adjacent to the monolayers were equal to the applied concentrations.

The density of bound F-(ANO2 Fab) was calculated from the measured ratio

$$\frac{C}{Ad} = \frac{\beta_1 F_1}{[1 - \beta_2]F_2} \tag{3}$$

where β_1 and β_2 and F_1 and F_2 were the bleachable fractions and the mean fluorescence intensities of F-(ANO2 Fab) on DNP-cap-DPPE/DPPC monolayers in the absence and presence of 100 μM DNP-G, respectively (Pearce et al., 1992; Poglitsch et al., 1991). The measured parameter values for $A = 2.6$ μM and $d = 820$ Å were $\beta_1 \approx 0.95$, $\beta_2 \approx 0.85$, and $F_1/F_2 \approx 5$, so that $C \approx 4{,}100$ molecules/μm^2. This value together with the measured value of K implies that the density of F-(ANO2 Fab) on DNP-cap-DPPE/DPPC monolayers at saturation would be $N \approx 13{,}800$ molecules/μm^2.

Surface binding kinetics of F-(ANO2 Fab) on supported monolayers

TIR-FPR was used to investigate the kinetics of F-(ANO2 Fab) binding to DNP-cap-DPPE/DPPC monolayers. The characteristic times of TIR-FPR recovery curves for F-(ANO2 Fab) on DNP-cap-DPPE/DPPC monolayers were on the order of seconds and the recovery was nearly complete after 30 s (Fig. 2).

The TIR-FPR recovery curves were analyzed with a multi-exponential function, i.e.,

$$F(t) = F(-) + [F(0) - F(-)] \sum_{i=0}^{n} r_i e^{-k_i t} \tag{4a}$$

$$1 = \sum_{i=0}^{n} r_i \tag{4b}$$

where $F(-)$ was the known prebleach fluorescence, k_0 was assumed to equal zero, n was the number of reversible components (which varied from one to three), and the $2n + 1$ free parameters were $F(0)$, r_i, and k_i (for $i = 1$ to n). The fraction of bound, bleached F-(ANO2 Fab) that did not exchange with solution phase F-(ANO2 Fab) during the time range of fluorescence recovery, r_0, was calculated from the best-fit values of r_i (for $i = 1$ to n) and Eq. 4b.

TIR-FPR recovery curves were not well fit by Eq. 4 with one reversible component ($n = 1$), but could be adequately fit by this equation with either two ($n = 2$) or three ($n = 3$) reversible components. The mean value of the F-statistic of the chi-squared goodness-of-fit parameter for comparing the one- and two-component fits was 116, well above the critical value of 3 (Wright et al., 1988), whereas the mean F-statistic for comparing the two- and three-component fits was ≈ 1. Therefore, the data were best described by two reversible components. The best-fit values of the two rates, k_1 and k_2, their associated fractional recoveries, r_1 and r_2, and the irreversible fraction, r_0, are shown in Table 2 for different sample types.

The best-fit parameters for TIR-FPR recovery curves changed little when the duration of the bleach pulse was changed by a factor of four, from 50 to 200 ms. Overall, the magnitudes of the rates k_1 and k_2 changed by <20% (e.g., from 0.10 to 0.08 s^{-1}) and the fractional recoveries changed by <5% (e.g., from 0.50 to 0.48). This result argues against the presence of photo-induced artifacts such as the formation of covalent crosslinks between surface bound proteins (e.g., Sheetz and Koppel, 1979) and demonstrates that the bleaching pulse was short enough to be effectively infinitesimal.

TIR-FPR recovery curves for simple bimolecular surface reactions

Previous theoretical work (Thompson et al., 1981) has shown that, for the simple binding mechanism shown in

TABLE 2 TIR-FPR rates and fractional recoveries

[Fab] (μM)	Area (μm × μm)	k_1 (s^{-1})	k_2 (s^{-1})	r_1	r_2	r_0
1	50 × 200	0.11 ± 0.01	1.22 ± 0.16	0.35 ± 0.03	0.48 ± 0.02	0.17 ± 0.03
3	50 × 200	0.10 ± 0.01	1.31 ± 0.16	0.31 ± 0.04	0.49 ± 0.04	0.20 ± 0.04
5	50 × 200	0.11 ± 0.01	1.13 ± 0.02	0.32 ± 0.01	0.47 ± 0.02	0.21 ± 0.01
10	50 × 200	0.11 ± 0.01	1.23 ± 0.04	0.29 ± 0.01	0.52 ± 0.01	0.18 ± 0.01
1	200 × 550	0.09 ± 0.02	1.17 ± 0.17	0.37 ± 0.01	0.47 ± 0.02	0.16 ± 0.02
10	200 × 550	0.10 ± 0.01	1.21 ± 0.04	0.29 ± 0.01	0.54 ± 0.01	0.17 ± 0.01

The best-fit values of the off rates, k_1 and k_2, and the fractional recoveries, r_0, r_1 and r_2, were not significantly different for four different F-(ANO2 Fab) solution concentrations or for different illumination areas. Each value is the mean and standard error in the mean of 3–45 recovery curves from three to five independently prepared DNP-cap-DPPE/DPPC monolayers.

Eq. 1a and for a large illuminated area, the form of the TIR-FPR recovery curve is a rather complex function that depends on the intrinsic dissociation rate, k_{off}, and a transport rate, R_N, where

$$R_N = \frac{D_{soln}(1 + KA)^2}{(KN)^2} \quad (5)$$

and D_{soln} is the ligand diffusion coefficient in solution. R_N is the rate of transport in solution through a slab of thickness C/A, which gives the depth of a layer next to the surface that contains a two-dimensional density of unbleached molecules sufficient to replace the density of surface-bound, bleached molecules. If $k_{off} \gg R_N$, then TIR-FPR recovery curves are predicted to be "diffusion limited." In this case, the recovery curve depends only on R_N and is not monoexponential, and the recovery rate changes with the F-(ANO2 Fab) solution concentration, A, as shown in Eq. 5. If $k_{off} \ll R_N$, the recovery curve is "reaction limited" and is a single exponential with rate k_{off}, and the recovery rate is independent of the ligand solution concentration.

For $K = 1.6 \times 10^5\ M^{-1}$, $D_{soln} = 5 \times 10^{-7}\ cm^2/s$, $N =$ 13,800 molecules/μm^2, and A = 1–10 μM, R_N ranges from 5 to 25 s^{-1}. These values are higher than the observed recovery rates, $k_{off} \approx 0.1$–$1\ s^{-1}$, suggesting that the TIR-FPR data are reaction limited. The data were independent of the F-(ANO2 Fab) solution concentration over a range that corresponded to a fractional surface site saturation of 14–62% (for A = 1–10 μM), confirming that the recovery curves were reaction limited.

In theory, another fundamental transport rate may also affect TIR-FPR data (Thompson et al., 1981). This rate is related to the semi-minor axis of the illuminated elliptical area, denoted by s, and equals

$$R_L = \frac{D_{soln}}{s^2} \quad (6)$$

For $s \geq 25\ \mu m$ and $D_{soln} \approx 5 \times 10^{-7}\ cm^2/s$, $R_L \leq 0.08\ s^{-1}$, which is only slightly lower than the observed fluorescence recovery rate. However, in cases where the transport process associated with R_L plays a role in the fluorescence recovery, the observed recovery rate should be strongly dependent on the size of the illuminated area, but the TIR-FPR recovery curves for F-(ANO2 Fab) on DNP-cap-DPPE/DPPC monolayers did not measurably change when the semi-minor axis of the elliptical illuminated area was changed by a factor of four (Table 2). Thus, because $R_N > R_L$, replenishment of surface-bound, bleached molecules occurred primarily through solution diffusion normal to the interface (R_N) and diffusion lateral to the interface (R_L) did not limit the rate of fluorescence recovery.

If surface-bound, fluorescently labeled ligand undergoes diffusion along the surface, a third transport rate may affect the rate of fluorescence recovery. This rate is given by

$$R_S = \frac{D_{surf}}{s^2} \quad (7)$$

where D_{surf} is the diffusion coefficient of membrane-bound ligand. The maximum surface diffusion coefficient of bound F-(ANO2 Fab) may be estimated as the lipid diffusion coefficient ($\leq 10^{-10}\ cm^2/s$) and $s \geq 25\ \mu m$, so that $R_S \leq 2 \times 10^{-5}$ s. Thus, R_S is much slower than the observed rate of fluorescence recovery. This calculation, together with the observation that the fluorescence recovery curves did not change with the size of the illuminated area, indicates that potential translational mobility of F-(ANO2 Fab) along the membrane surface was negligibly slow. This result rules out modes of translational mobility in which Fabs move rapidly over the lipid surface or move by fast and sequential membrane dissociation and association.

In the limit where the transport rates do not affect the rate of fluorescence recovery, the shape of the TIR-FPR recovery curve for the simple mechanism shown in Eq. 1a is a single exponential, i.e., $F(t)$ is given by Eqs. 4a and 4b with $n = 1$ and $r_0 = 0$ (Thompson et al., 1981). Therefore, because the observed data were not monoexponential with time, the association of F-(ANO2 Fab) with DNP-cap-DPPE/DPPC monolayers must involve a more complex surface binding mechanism. A possible explanation for the observed nonmonoexponential TIR-FPR recovery curves is considered below.

The measured dissociation rates for F-(ANO2 Fab) on DNP-cap-DPPE/DPPC monolayers were $k_1 \approx 0.1$ s^{-1} and $k_2 \approx 1$ s^{-1} (Table 2). These dissociation kinetic rates are much slower than those previously measured for ANO2 Fab with DNP-diglycine in solution ($k_{off} \approx$ 100 s^{-1}; Theriault et al., 1991). This comparison suggests that the mechanism for the association of ANO2 Fabs with haptens on membrane surfaces differs significantly from the mechanism for interaction with haptens in solution.

The apparent dissociation rates, together with the measured apparent association constant $K \approx 10^5$ M^{-1}, imply an apparent on rate of 10^4–10^5 M^{-1} s^{-1}. This value is much lower than that previously measured for ANO2 Fabs and DNP-diglycine in solution (Theriault et al., 1991) and than theoretical estimates for the diffusion-limited on rate for a protein ligand with a small molecule in solution or on a membrane surface (Berg and von Hippel, 1985). Similarly low values of apparent on rates have recently been measured for epidermal growth factor on cell membranes (2×10^6 M^{-1} s^{-1}; Hellen and Axelrod, 1991) and for bovine prothrombin fragment 1 on model membranes (10^5 M^{-1} s^{-1}; Pearce et al., 1992). On rate values that are much lower than the upper limit set by transport theory imply that a large fraction of the collisional encounters between protein molecules in solution and the membrane surface do not result in successful membrane binding.

Multiple conformations of bound antibodies

One possible explanation for the observed multi-exponential TIR-FPR recovery curves for F-(ANO2 Fab) on DNP-cap-DPPE/DPPC monolayers is that the bound F-(ANO2 Fab) assume more than one membrane-bound state. This type of Fab-hapten binding mechanism has previously been suggested for Fab-hapten kinetics in solution (Voss, 1990; Kranz et al., 1982; Denizot et al., 1979; Pecht and Lancet, 1977; Maeda et al., 1977). In this mechanism,

$$A + B \underset{k_{off}(1)}{\overset{k_{on}(1)}{\rightleftharpoons}} I \underset{k_{off}(2)}{\overset{k_{on}(2)}{\rightleftharpoons}} C \tag{8a}$$

$$K_1 = \frac{k_{on}(1)}{k_{off}(1)} = \frac{I}{AB} \tag{8b}$$

$$K_2 = \frac{k_{on}(2)}{k_{off}(2)} = \frac{C}{I} \tag{8c}$$

$$K = K_1(K_2 + 1) \tag{8d}$$

where I is a bound intermediate, $k_{on}(i)$ and $k_{off}(i)$ are kinetic rates, the K_i are association constants, and K is the apparent association constant. For this mechanism, the equilibrium binding data would be of the shape given in Eq. 2 and the reaction-limited TIR-FPR fluorescence recovery curves would be of the shape given in Eqs. 4a and 4b with $n = 2$ and $r_0 = 0$ (Hsieh and Thompson, unpublished results). Neglecting the irreversible fraction r_0,

$$\frac{r_1}{r_1 + r_2} = \frac{[k_1 - \rho][k_{off}(1) - k_2]}{[k_1 - k_2][k_{off}(1) - \rho]} \tag{9a}$$

$$2k_{1,2} = \rho \pm \sqrt{\rho^2 - 4k_{off}(1)k_{off}(2)} \tag{9b}$$

$$\rho = k_{off}(1) + k_{on}(2) + k_{off}(2) \tag{9c}$$

Algebraic manipulation of Eqs. 8 and 9 shows that the measured apparent association constant $K \approx 1.6 \times 10^5$ M^{-1} s^{-1} and kinetic parameters $k_1 \approx 0.11$ s^{-1}, $k_2 \approx 1.2$ s^{-1}, $r_1 \approx 0.32$, and $r_2 \approx 0.49$ (Table 2) may be used to calculate the kinetic rates and dissociation constants shown in Eqs. 8a–8c by the following procedure: $\rho \approx 1.3$ s^{-1} is the sum of $k_1 + k_2$ (Eq. 9b); $k_{off}(1) \approx 1.1$ s^{-1}, $k_{off}(2) \approx 0.12$ s^{-1}, and $k_{on}(2) \approx 0.056$ s^{-1} are obtained by sequentially inverting Eqs. 9a, 9b, and 9c, respectively; $K_2 \approx 0.48$ and $K_1 \approx 1.1 \times 10^5$ M^{-1} are calculated from Eqs. 8c and 8d, respectively; and $k_{on}(1) \approx 1.2 \times 10^5$ M^{-1} s^{-1} is then obtained from Eq. 8b.

For this mechanism, the data imply that the faster observed rate corresponds to dissociation of F-(ANO2 Fab) in the intermediate state, I, from the membrane and that the slower rate corresponds to conversion, on the membrane, of F-(ANO2 Fab) from state C to state I, followed by a more rapid membrane dissociation. The association constant K_2 for conversion between states I and C is approximately equal to one, which means that the bound F-(ANO2 Fab) are distributed in approximately equal amounts between the two bound states.

Other mechanisms

The presence of an impurity in the Fab preparations, which could in theory give rise to the observed nonmonoexponential surface binding kinetics, is not likely. Nondenaturing SDS-PAGE of overloaded gels that were visualized by silver staining showed that the Fab preparations were at least 97% pure. The primary "impurity" was of low molecular weight (≈25 kD) and appeared to be an artifact caused by the SDS in which the ANO2 light chain and heavy chain fragments ran separately from the intact ANO2 Fab. Furthermore, no amount of contaminating, intact ANO2 was detectable. The measured apparent association constant of tetramethylrhodamine-labeled intact ANO2 on DNP-cap-DPPE/DPPC monolayers is only 10-fold higher than that of tetramethylrhodamine-labeled, ANO2 Fab (Pisarchick and Thompson, 1990). Therefore, a fractional impurity of <1% intact ANO2 could not contribute significantly to the measured TIR-FPR recovery curves.

Another possible explanation for the nonmonoexponential TIR-FPR recovery curves is that the DNP-cap-DPPE/DPPC membrane surfaces contain two different types of antibody binding sites. The two binding site types could arise from different physical dinitrophenyl orientations; for example, coexistent lipid domains have previously been observed in single phospholipid mono-

layers (e.g., Seul et al., 1985; McConnell et al., 1984), and if such a domain structure existed in DNP-cap-DPPE/DPPC monolayers the different domains could present hapten to ANO2 Fab with different efficiencies. Different binding site types might in general also be related to the observation that some F-(ANO2 Fab) may bind to DNP-cap-DPPE/DPPC monolayers even when the hapten-binding regions are fully occupied by DNP-G from solution, i.e., the F-(ANO2 Fab) might bind both "specifically" and "nonspecifically" to the membrane surfaces.

The predicted shape of the equilibrium binding curve for the case in which the membrane surfaces contain different binding site types is not of the form of Eq. 2, but instead contains components related to the different association constants for reaction with the different surface sites types (Pearce et al., 1992). Thus, the TIR-FPR data would imply within this model of multiple binding site types that the monolayers have three types of binding sites with approximately equivalent abundances, where two site types had measurable dissociation rates ($\approx$ seconds) and one had a very slow dissociation rate (> minutes). However, consistency with the equilibrium data could be maintained only if the association constants for the three site types were approximately equal, so that the different off rate magnitudes were offset by correspondingly different on rate magnitudes. Previous work has shown that the equilibrium binding curve for tetramethylrhodamine-labeled ANO2 Fab is well described by Eq. 2 and does not contain components with different association constants (Pisarchick and Thompson, 1990). Thus, the mechanism of multiple binding sites types is considered to be unlikely.

Another plausible explanation for the observed nonmonoexponential TIR-FPR recovery curves is that the DNP groups on the surfaces of the DNP-cap-DPPE/DPPC monolayers maintain a dynamic equilibrium between antibody accessible and inaccessible states. This phenomenon has previously been observed for anti-hapten antibodies and phospholipid vesicles that contain hapten-conjugated phospholipids (Stanton et al., 1984; Petrossian and Owicki, 1984; Balakrishnan et al., 1982*b*). However, for this mechanism, reaction-limited TIR-FPR recovery curves would be monoexponential in shape (Hsieh and Thompson, unpublished results).

Two prior reports at first suggest that direct interactions between F-(ANO2 Fab) in solution or on the membrane surface might give rise to the observed nonmonoexponential surface kinetics. First, the ability of membrane-bound bivalent antibodies to form two-dimensional crystals is well documented (e.g., Uzgiris and Kornberg, 1983; Uzgiris, 1986), and one previous work has suggested that intermediate states in which membrane-bound antibodies are arranged in small clusters may exist (Wright et al., 1988). Although in theory attractive or repulsive interactions among monolayer-bound Fab or Fab-phospholipid complexes could give rise to complex kinetic recovery curves, this possibility is considered unlikely because the data do not depend on the antibody solution concentration and therefore do not depend on the antibody surface density. Second, the ANO2 antibody appears to be an auto-antibody so ANO2 Fabs can form dimers in solution (Theriault et al., 1991); however, the dimers occur only at concentrations $\geq 100\ \mu M$, well above the solution concentration of F-(ANO2 Fab) used in this work. Finally, a mechanism in which the nonmonoexponential kinetics result from decreased on rates at high F-(ANO2 Fab) surface densities, due to a putative reshuffling of bound F-(ANO2 Fab) that might be required to produce new binding sites, is also considered to be unlikely because the data do not depend on the F-(ANO2 Fab) surface density.

SUMMARY

This work is one of the first demonstrations of TIR-FPR as a method for measuring the dissociation kinetics of fluorescently labeled protein ligands at specific sites on model membrane surfaces. The data demonstrate that this technique can yield quantitative kinetic data for protein-membrane association processes. The results show that, for F-(ANO2 Fab) on DNP-cap-DPPE/DPPC membranes, the fluorescence recovery curves are reaction limited, and therefore contain information about the intrinsic dissociation process rather than solution transport. In addition, the recovery curves are not monoexponential and the measured kinetic rate constants are much different from those for ANO2 Fab with dinitrophenylated haptens in solution, implying that the F-(ANO2 Fab) does not interact with DNP groups on the membrane surface via a simple, reversible bimolecular reaction. Future investigations may provide a more thorough understanding of the conversion between monovalent and bivalent attachment of antibodies at membrane surfaces (Pisarchick and Thompson, 1990), the role of these kinetics in the lateral (Wright et al., 1988) and rotational (Timbs and Thompson, 1990) mobility of bound antibodies, and the mechanism by which bound antibodies on planar model membrane surfaces form two-dimensional crystals (Uzgiris and Kornberg, 1983).

We thank Kenneth H. Pearce for many helpful discussions. This work was supported by National Institutes of Health grant GM-37145 (N.L.Thompson), National Science Foundation grant DCB-8552986 (N.L.Thompson), and a Department of Education Graduate Fellowship (D.Gesty).

Received for publication 23 December 1991.

REFERENCES

Abney, J. R., B. A. Scalettar, and N. L. Thompson. 1992. Evanescent interference patterns for fluorescence microscopy. *Biophys. J.* 61:542–552.

Axelrod, D., T. P. Burghardt, and N. L. Thompson. 1984. Total internal reflection fluorescence. *Annu. Rev. Biophys. Bioeng.* 13:247–268.

Axelrod, D., R. M. Fulbright, and E. H. Hellen. 1986. Adsorption kinetics on biological membranes: measurement by total internal reflection fluorescence. *In* Applications of Fluorescence in the Biomedical Sciences. D. L. Taylor, A. S. Waggoner, F. Lanni, R. F. Murphy, and R. Birge, editors. Alan R. Liss, New York. 461–476.

Balakrishnan, K., F. J. Hsu, D. G. Hafeman, and H. M. McConnell. 1982*a*. Monoclonal antibodies to a nitroxide lipid hapten. *Biochim. Biophys. Acta.* 721:30–38.

Balakrishnan, K., S. Q. Mehdi, and H. M. McConnell. 1982*b*. Availability of dinitrophenylated lipid haptens for specific antibody binding depends on the physical properties of host bilayer membranes. *J. Biol. Chem.* 257:6434–6439.

Berg, O. G., and P. H. von Hippel. 1985. Diffusion-controlled macromolecular interactions. *Annu. Rev. Biophys. Biophys. Chem.* 14:131–160.

Burghardt, T. P., and D. Axelrod. 1981. Total internal reflection/fluorescence photobleaching recovery study of serum albumin adsorption dynamics. *Biophys. J.* 33:455–468.

Darst, S. A., C. R. Robertson, and J. A. Berzofsky. 1988. Adsorption of the protein antigen myoglobin affects the binding of conformation specific monoclonal antibodies. *Biophys. J.* 53:533–539.

Denizot, F. C., M. H. Hirn, and M. A. DeLaage. 1979. Relationship between affinity and kinetics in a hapten-antibody reaction. Studies on anti-cyclic AMP antibodies. *Molec. Immunol.* 16:509–513.

Hafeman, D. G., V. von Tscharner, and H. M. McConnell. 1981. Specific antibody-dependent interactions between macrophages and lipid haptens in planar lipid monolayers. *Proc. Natl. Acad. Sci. USA* 78:4552–4556.

Hellen, E. H., R. M. Fulbright, and D. Axelrod. 1988. Total internal reflection fluorescence: theory and applications at biosurfaces. *In* Spectroscopic Membrane Probes. L. M. Loew, editor. CRC Press, Boca Raton. 47–79.

Hellen, E. H., and D. Axelrod. 1991. Kinetics of epidermal growth factor/receptor binding on cells measured by total internal reflection/fluorescence photobleaching recovery. *J. Fluorescence.* 2:113–128.

Hlady, V., J. Rickel, and J. D. Andrade. 1988/1989. Fluorescence of adsorbed protein layers. II. Adsorption of human lipoproteins studied by total internal reflection intrinsic fluorescence. *Colloids Surf.* 34:171–183.

Kalb, E., J. Engel, and L. K. Tamm. 1990. Binding of proteins to specific target sites in membranes measured by total internal reflection microscopy. *Biochemistry.* 29:1607–1613.

Kimura, K., M. Nakanishi, M. Ueda, J. Ueno, H. Nariuchi, S. Furakawa, and T. Yasuda. 1986. The effect of immunoglobulin G1 structure on macrophage binding to supported planar lipid monolayers. *Immunology.* 59:235–238.

Kranz, D. M., J. N. Herron, and E. W. Voss. 1982. Mechanisms of ligand binding by monoclonal anti-fluorescyl antibodies. *J. Biol. Chem.* 257:6987–6995.

Maeda, H., A. Schmidt-Kessen, J. Engel, and J-C. Jaton. 1977. Kinetics of binding of oligosaccharides to a homogeneous pneumococcal antibody: dependence on antigen chain length suggest a labile intermediate complex. *Biochemistry.* 16:4086–4089.

Mahan, A. I., and C. V. Bitterli. 1978. Total internal reflection: a deeper look. *Applied Optics.* 17:509–519.

McConnell, H. M., L. Tamm, and R. Weis. 1984. Periodic structures in lipid phase transitions. *Proc. Natl. Acad. Sci. USA.* 81:3249–3253.

McConnell, H. M., T. H. Watts, R. M. Weis, and A. A. Brian. 1986. Supported planar membranes in studies of cell–cell recognition in the immune system. *Biochim. Biophys. Acta.* 864:95–106.

Pearce, K. H., R. G. Hiskey, and N. L. Thompson. 1992. Surface binding kinetics of prothrombin fragment 1 on planar membranes measured by total internal reflection fluorescence microscopy. *Biochemistry.* In press.

Pecht, I., and D. Lancet. 1977. Kinetics of antibody-hapten interactions. *In* Chemical Relaxation in Molecular Biology. I. Pecht and R. Rigler, editors. Springer-Verlag, Berlin. 306–338.

Petrossian, A., and J. C. Owicki. 1984. Interactions of antibodies with liposomes bearing fluorescent haptens. *Biochim. Biophys. Acta.* 776:217–227.

Piepenstock, M., M. Lösche, and H. Möhwald. 1991. Local control of antibody binding to hapten presenting interfaces: steric and electrostatic interactions. *Biophys. J.* 59:626*a*.(Abstr.)

Pisarchick, M. L., and N. L. Thompson. 1990. Binding of a monoclonal antibody and its Fab fragment to supported phospholipid monolayers measured by total internal reflection fluorescence microscopy. *Biophys. J.* 58:1235–1249.

Poglitsch, C. L., and N. L. Thompson. 1990. Interaction of antibodies with Fc receptors in substrate-supported planar membranes measured by total internal reflection fluorescence microscopy. *Biochemistry.* 29:248–254.

Poglitsch, C. L., M. T. Sumner, and N. L. Thompson. 1991. Binding of IgG to moFcγ RII purified and reconstituted into supported planar membranes as measured by total internal reflection fluorescence microscopy. *Biochemistry.* 30:6662–6671.

Schmidt, C. F., R. M. Zimmerman, and H. E. Gaub. 1990. Multilayer adsorption of lysozyme on a hydrophobic substrate. *Biophys. J.* 57:577–588.

Seul, M., S. Subramaniam, and H. M. McConnell. 1985. Mono- and bilayers of phospholipids at interfaces: interlayer coupling and phase stability. *J. Phys. Chem.* 89:3592–3595.

Sheetz, M. P., and D. E. Koppel. 1979. Membrane damage caused by irradiation of fluorescent concanavalin A. *Proc. Natl. Acad. Sci. USA.* 76:3314–3317.

Stanton, S., A. Kantor, A. Petrossian, and J. C. Owicki. 1984. Location and dynamics of a membrane-bound fluorescent hapten: a spectroscopic study. *Biochim. Biophys. Acta.* 776:228–236.

Subramaniam, S., M. Seul, and H. M. McConnell. 1986. Lateral diffusion of specific antibodies bound to lipid monolayers on alkylated substrates. *Proc. Natl. Acad. Sci. USA.* 83:1169–1173.

Sui, S., T. Urumow, and E. Sackmann. 1988. Interaction of insulin receptors with lipid bilayers and specific and nonspecific binding of insulin to supported membranes. *Biochemistry.* 27:7463–7469.

Tamm, L. K. 1988. Lateral diffusion and fluorescence microscope studies on a monoclonal antibody specifically bound to supported phospholipid bilayers. *Biochemistry.* 27:1450–1457.

Tendian, S. W., B. R. Lentz, and N. L. Thompson. 1990. Calcium-independent binding of prothrombin to negatively charged planar membranes detected by total internal reflection fluorescence microscopy. *Biochemistry.* 30:10991–10999.

Theriault, T. P., D. J. Leahy, M. Levitt, H. M. McConnell, and G. S. Rule. 1991. Structural and kinetic studies of the Fab fragment of a monoclonal anti-spin label antibody by NMR. *J. Mol. Biol.* 221:257–270.

Thompson, N. L., T. P. Burghardt, and D. Axelrod. 1981. Measuring surface dynamics of biomolecules by total internal reflection fluorescence with photobleaching recovery or correlation spectroscopy. *Biophys. J.* 33:435–454.

Thompson, N. L., A. G. Palmer, L. L. Wright, and P. E. Scarborough. 1988. Fluorescence techniques for supported planar model membranes. *Comm. Molec. Cell. Biophys.* 5:109–131.

Tilton, R. D., A. P. Gast, and C. R. Robertson. 1990*a*. Surface diffusion of interacting proteins: effect of concentration on the lateral mobility of adsorbed bovine serum albumin. *Biophys. J.* 58:1321–1326.

Tilton, R. D., C. R. Robertson, and A. P. Gast. 1990*b*. Lateral diffusion

of bovine serum albumin adsorbed at the solid-liquid interface. *J. Colloid Interface Sci.* 137:192–203.

Timbs, M. M., and N. L. Thompson. 1990. Slow rotational mobilities of antibodies and lipids associated with substrate-supported phospholipid monolayers as measured by polarized fluorescence photobleaching recovery. *Biophys. J.* 58:413–428.

Timbs, M. M., C. L. Poglitsch, M. L. Pisarchick, M. T. Sumner, and N. L. Thompson. 1991. Binding and mobility of anti-dinitrophenyl monoclonal antibodies on fluid-like, Langmuir-Blodgett phospholipid monolayers containing dinitrophenyl-conjugated phospholipids. *Biochim. Biophys. Acta.* 1064:219–228.

Uzgiris, E. E., and R. D. Kornberg. 1983. Two-dimensional crystallization technique for imaging macromolecules, with application to antigen-antibody-complement complexes. *Nature (Lond.).* 301:125–129.

Uzgiris, E. E. 1986. Supported phospholipid bilayers for two-dimensional protein crystallization. *Biochem. Biophys. Res. Comm.* 134:819–826.

Voss, E. W. 1990. Anti-fluorescyl antibodies as structure-function models to examine fundamental immunochemical and spectroscopic principles. *Comm. Molec. Cell. Biophys.* 5:197–221.

Weis, R. M., K. Balakrishnan, B. A. Smith, and H. M. McConnell. 1982. Stimulation of fluorescence in a small contact region between rat basophil leukemia cells and planar lipid membrane targets by coherent evanescent radiation. *J. Biol. Chem.* 257:6440–6445.

Wright, L. L., A. G. Palmer, and N. L. Thompson. 1988. Inhomogeneous translational diffusion of antibodies specifically bound to phospholipid Langmuir-Blodgett films. *Biophys. J.* 54:463–470.

Zimmerman, R. M., C. F. Schmidt, and H. E. Gaub. 1990. Absolute quantities and equilibrium kinetics of macromolecular adsorption measured by fluorescence photobleaching in total internal reflection. *J. Colloid Interface Sci.* 139:268–280.